Structure and Interactions of the Helical and U-Box Domains of CHIP, the C Terminus of HSP70 Interacting Protein[†,‡]

Zhen Xu,[§] Karl I. Devlin,[§] Michael G. Ford,[§] Jay C. Nix,[||] Jun Qin,[§] and Saurav Misra*[,§]

Department of Molecular Cardiology, The Cleveland Clinic Foundation, Cleveland, Ohio 44195, and Molecular Biology Consortium, Advanced Light Source Beamline 4.2.2, Lawrence Berkeley National Laboratory, Berkeley, California 94720

Received January 24, 2006; Revised Manuscript Received February 24, 2006

ABSTRACT: The heat-shock proteins Hsp70 and Hsp90 play a crucial role in regulating protein quality control both by refolding and by preventing the aggregation of misfolded proteins. It has recently been shown that Hsp70 and Hsp90 act not only in protein refolding but also cooperate with the C terminus of Hsp70 interacting protein (CHIP), a multidomain ubiquitin ligase, to mediate the degradation of unfolded proteins. We present the crystal structure of the helical linker domain and U-box domain of zebrafish CHIP (*Dr*CHIP-HU). The structure of *Dr*CHIP-HU shows a symmetric homodimer. The conformation of the helical linker domains and the relative positions of the helical and U-box domains differ substantially in *Dr*CHIP-HU from those in a recently published structure of an asymmetric dimer of mammalian (mouse) CHIP. We used an in vitro ubiquitination assay to identify residues, located on two long loops and a central α helix of the CHIP U-box domain, that are important for interacting with the ubiquitin-conjugating enzyme UbcH5b. In addition, we used NMR spectroscopy to define a complementary interaction surface located on the N-terminal α helix and the L4 and L7 loops of UbcH5b. Our results provide insights into conformational variability in the domain arrangement of CHIP and into U-box-mediated recruitment of UbcH5b for the ubiquitination of Hsp70 and Hsp90 substrates.

The heat-shock proteins Hsc/Hsp70 and Hsp90 are versatile molecular chaperones that mediate a wide variety of cellular processes under quiescent conditions and under conditions of cellular stress (*1*, *2*). These chaperones shield hydrophobic epitopes on nascent native proteins, helping to maintain the proper conformations of these proteins. They also prevent the aggregation and enable the refolding of destabilized, unfolded, or misfolded proteins (*1*). Hsc70 is present under basal conditions, while its homologue Hsp70 is transcriptionally upregulated after heat shock. Both bind reversibly to substrate proteins in an ATP-dependent manner, cycling between high-substrate affinity ADP-bound states and low-affinity ATP-bound states (*3*). Hsp90 is a dimeric chaperone that, among other functions, stabilizes the native conformations of many signaling proteins, including nuclear hormone receptors and protein kinases (*3*, *4*). Both chaperones are regulated by cochaperones that modulate their substrate affinities and refolding kinetics and link the chaperones to other cellular pathways (*3*).

The C terminus of Hsp70 interacting protein (CHIP)[1] is a recently identified cochaperone that links Hsc/Hsp70 and Hsp90 to protein degradation (*5*−*9*), a function that is complementary to protein stabilization and refolding in protein quality control (*10*, *11*). The degradation of cytoplasmic proteins is associated with the addition of a K48-linked polyubiquitin chain to a lysine side chain of the substrate by the cooperative actions of E1 (ubiquitin-activating enzyme), E2 (ubiquitin-conjugating enzyme), and E3 (ubiquitin ligase) enzymes (*12*, *13*). The polyubiquitin chain targets the modified protein for degradation by the proteasome (*12*, *14*). E3 ligases lend specificity to ubiquitination by functioning as adapters between E2 enzymes, which are covalently attached to ubiquitin, and specific protein targets. E3 ligases that contain homologous to E6-AP carboxy terminus (HECT) domains become transiently attached to the ubiquitin through a thioester bond during the transfer of the ubiquitin from the E2 enzyme to the substrate. Ligases that contain zinc-finger really interesting new gene (RING) domains enable the direct transfer of the ubiquitin from the E2 enzyme to the substrate lysine side chain without becoming transiently modified (*15*, *16*).

CHIP is a multidomain E3 ligase that consists of an N-terminal tetratricopeptide repeat (TPR) domain, a linker domain that was predicted to be primarily helical, and a C-terminal U-box domain (*17*). The TPR domain of CHIP

[†] S.M. is supported by funding from the Cleveland Clinic Foundation. The Advanced Light Source is supported by the U.S. DOE under contract number DE-AC03-76SF00098 at Lawrence Berkeley National Laboratory.

[‡] Coordinates and structure factors have been deposited in the Protein Data Bank as entry 2F42.

* To whom correspondence should be addressed. Telephone: (216) 444-2054. Fax: (216) 445-8204. E-mail: misras@ccf.org.

[§] Cleveland Clinic Foundation.

[||] Lawrence Berkeley National Laboratory.

[1] Abbreviations: CHIP, C terminus of Hsp70-interacting protein; *Dr*CHIP-HU, zebrafish CHIP helical linker and U-box domains; *Mm*CHIP, mouse CHIP; *Hs*CHIP, human CHIP; TPR, tetratricopeptide repeat; E1, ubiquitin-activating enzyme; E2, ubiquitin-conjugating enzyme; E3, ubiquitin ligase; E4, polyubiquitin chain extension enzyme; RING finger, really interesting new gene zinc-finger domain; HECT, homologous to E6-AP carboxy terminus; GST, glutathione *S*-transferase; TEV protease, tobacco etch virus protease; SAD, single-wavelength anomalous diffraction.

10.1021/bi0601508 CCC: $33.50
Published on Web 03/23/2006

binds directly to ΦEEVD motifs located at the C termini of Hsc/Hsp70 and Hsp90, where Φ denotes a large hydrophobic residue (*17*−*19*). U-Box domains possess E3 ubiquitin ligase activity and, in some contexts, polyubiquitin chain extension enzyme (E4) activity (*20*−*22*). U-Box domains are structurally similar to RING domains but are stabilized by two sets of hydrogen-bonding networks in positions analogous to the locations of the stabilizing zinc ions in RING domains (*23*−*25*). When bound to Hsp70 or Hsp90, CHIP recruits E2 enzymes of the Ubc4/UbcH5 family to ubiquitinate misfolded proteins that occupy the chaperone substrate-binding sites, thus remodeling the chaperones from protein-refolding complexes to complexes that promote degradation (*5*−*9*). The helical linker domain that connects the TPR and U-box domains is required for the proper functioning of CHIP (*26*), suggesting that the TPR and helical domains play a crucial role in properly positioning the U-box domains in the context of a CHIP−chaperone heterocomplex.

CHIP−chaperone heterocomplexes target a diverse group of different chaperone substrates for degradation. These include members of the nuclear hormone receptor family (*17*, *27*−*31*), various kinases including the oncogenic receptor tyrosine kinase ErbB2 (*32*, *33*), members of the Smad family of TGF-β signal transducers (*34*−*36*), p53 (*37*), and the endocytic protein epsin (*38*). CHIP is particularly involved in the degradation and clearance of misfolded proteins that are prone to aggregation and the formation of intracellular inclusions. Expression of CHIP has a protective effect on the formation of intracellular aggregates by and promotes the clearance of such aggregate-forming proteins as α-synuclein (*39*), expanded polyglutamine repeat-huntingtin and ataxin-3 (*40*, *41*), Tau protein (*42*−*44*), familial amyotrophic lateral sclerosis mutants of superoxide dismutase-1 (*45*, *46*), and the cystic fibrosis transmembrane-conductance regulator (CFTR) (*47*, *48*). These proteins are all implicated in severe pathologies of the nervous system or other diseases. Because CHIP also regulates the degradation of proteins such as ErbB2 (*32*, *33*) that are directly involved in cancer, CHIP may have potential as a target for amelioration of disease states through the modulation of the protein quality control system.

To further understand the mechanisms by which CHIP functions in chaperone-associated ubiquination, we have crystallized and solved the structure of a construct containing the helical linker and U-box domains of zebrafish CHIP (*Dr*CHIP-HU). Shortly after deposition of our structure in the Protein Data Bank, a structure of the full-length mouse CHIP protein (*Mm*CHIP) was released (*49*). Both our structure and the structure of *Mm*CHIP show novel homodimeric assemblies, in which dimerization is mediated by both the helical linker and U-box domains. Our structure, however, is a symmetric dimer, while the crystal structure of *Mm*CHIP is an asymmetric dimer with a substantially different conformation. In addition, we have used site-directed mutagenesis and NMR spectroscopy to probe the interaction between CHIP and the E2 enzyme UbcH5b, a member of the class of E2 enzymes recruited by CHIP in vivo. We show that two long loops of the CHIP U-box interact with helix α1 and the L4 and L7 loops of UbcH5b, resembling the interaction of certain RING finger domains with their cognate E2 enzymes. Our results suggest that asymmetric dimerization is not an obligate conformation of CHIP and that CHIP may undergo conformational changes between symmetric and asymmetric forms.

EXPERIMENTAL PROCEDURES

Expression and Purification of Recombinant Proteins. Zebrafish (*Danio rerio*) CHIP residues 112−284 containing the linker and U-box domains (*Dr*CHIP-HU), and human CHIP (*Hs*CHIP) constructs were cloned from expressed sequence tag IMAGE clones 5409937 and 5409937 (American Type Culture Collection), respectively. *Dr*CHIP-HU and full-length *Hs*CHIP were cloned into pET151/D-TOPO (Invitrogen) and expressed as His-tagged fusion proteins in *Escherichia coli* Rosetta2(DE3) cells (Novagen) at 20 °C for 16 h after induction with 0.5 mM IPTG. Proteins were purified by nickel-affinity chromatography in buffers containing 50 mM sodium phosphate at pH 8.0 and 300 mM NaCl. The His tags were removed after overnight cleavage with tobacco etch virus (TEV) protease (*50*) using a second round of nickel-affinity chromatography. Additional purification was performed by gel-filtration or anion-exchange chromatography. The methionine auxotroph *E. coli* B834-(DE3) (Novagen) was used to express selenomethionylated *Dr*CHIP-HU in defined media supplemented with 40 mg/L selenomethionine. SeMet-*Dr*CHIP-HU was purified using the same protocol as the native protein, with the addition of 5 mM 2-mercaptoethanol to buffers.

Human UbcH5b was obtained from IMAGE clone 4827210. Human UbcH5b and the U-box of human CHIP (*Hs*CHIP-U, residues 224−303) were cloned into the vector pGST||2 (*51*). The resulting glutathione-*S*-transferase (GST) fusion proteins were expressed in Rosetta2(DE3) cells at 20 °C for 20 h after induction with 0.5 mM IPTG. GST-UbcH5b and GST-*Hs*CHIP-U were purified by glutathione-affinity chromatography using a GSTPrepFF column (GE Healthcare) in buffers containing 150 mM NaCl and 50 mM sodium phosphate at pH 8.0. GST tags were removed by overnight cleavage with TEV protease during dialysis in 100 mM NaCl, 50 mM sodium phosphate at pH 7.0, 5 mM 2-mercaptoethanol, and a second pass over the GSTPrepFF. ^{15}N-Labeled UbcH5b was expressed in minimal media with 1.1 g/L ($^{15}NH_4)_2SO_4$ and purified in the same manner as the unlabeled protein.

Crystallization, Data Collection, and Structure Solution of DrCHIP-HU. *Dr*CHIP-HU was dialyzed in 50 mM NaCl, 20 mM Tris-HCl (pH 7.4), and 2 mM DTT at 40−50 mg/mL. Native *Dr*CHIP-HU crystals were obtained using hanging-drop vapor diffusion over reservoirs containing 9% PEG 3350, 0.1 M Bis-Tris (pH 6.6), and 0.1 M LiCl. SeMet-*Dr*CHIP-HU crystals were obtained by streak seeding or microseeding of native crystals into SeMet-*Dr*CHIP-HU drops (at 25−50 mg/mL) equilibrated against 9−10% PEG 3350 and 0.1 M sodium citrate (pH 5.0−5.6). Seeds of the resulting SeMet-*Dr*CHIP-HU crystals were transferred to fresh SeMet-*Dr*CHIP-HU drops to obtain well-diffracting crystals. Native and SeMet crystals were cryoprotected by serial 5 min incubations in reservoir solution supplemented with 5, 10, 15, and 20% glycerol and frozen in liquid nitrogen. Native and single-wavelength anomalous diffraction (SAD) data sets complete to 2.5 and 2.9 Å, respectively, were collected at Advanced Light Source beamline 4.2.2., Lawrence Berkeley National Laboratory, Berkeley, CA.

Table 1: Crystallographic Data Collection and Refinement Statistics for *Dr*CHIP-HU

experimental data	native	SAD
space group	$P6_522$	$P6_522$
unit cell: a, b, c (Å)	100.5, 100.5, 74.31	100.23, 100.23, 76.07
α, β, γ (deg)	90, 90, 120	90, 90, 120
wavelength (Å)	1.2399	0.9786
resolution range (Å)	50.25−2.50 (2.59−2.50)[a]	38.04−2.90 (3.00−2.90)
unique reflections	8099	5367
mosaicity	1.21	1.43
redundancy	19.1 (19.0)	20.3 (21.3)
I/σ	24.5 (5.7)	18.6 (4.4)
completeness (%)	100 (100)	100 (100)
R_{merge} (%)[b]	5.2 (48.0)	8.9 (56.6)
refinement		
resolution range (Å)	50.25−2.50 (2.59−2.50)	
number of reflections	8008	
R factor (%)[c]	26.6	
free *R* factor (%)[d]	28.5	
number of protein atoms	1144	
number of water molecules	71	
number of other atoms	1	
B factors (Å^2)		
overall mean	72.7	
from Wilson plot	60.1	
bulk solvent model	55.2	
rmsd bond lengths (Å)	0.008	
rmsd bond angles (deg)	1.1	
rmsd dihedral angles (deg)	20.0	
rmsd improper angles (deg)	0.69	
Luzzati coordinate error (Å)	0.42	
Ramachandran plot (%)		
most favored and allowed	98.4	
generously allowed	1.6	

[a] Statistics in parentheses are for the highest resolution shell. [b] $R_{merge} = \sum|I_i - \langle I_i\rangle|/\sum|I_i|$. [c] *R* factor $= \sum_h||F_{obs}(h)|-k|F_{calc}(h)||/\sum_h F_{obs}(h)$. [d] The free *R* factor is the *R* factor calculated for 10% of reflections excluded from refinement.

Diffraction data were indexed, integrated, and scaled using D*TREK (*52*). Indexing, data reduction, and generation of experimental maps showed that *Dr*CHIP-HU crystallized in space group $P6_522$ with unit cell dimensions $a = 100.5$ Å, $b = 100.5$ Å, and $c = 74.3$ Å, with one *Dr*CHIP-HU molecule per asymmetric unit. Phasing and density modification were performed with SOLVE/RESOLVE (*53*, *54*) using the SAD data set. The experimental density map was used for model building in O (*55*). Refinement against the 2.5 Å native dataset and model rebuilding were carried out using CNS 1.1 (*56*) and O. The final model has an *R* factor of 26.6% and a free *R* factor of 28.5% with no Ramachandran violations. Crystallographic data, phasing, and refinement statistics are summarized in Table 1.

In Vitro Ubiquitination Assays. Site-directed mutations were introduced into full-length His-tagged *Hs*CHIP using the QuickChange mutagenesis kit (Stratagene) and verified by sequencing. Mutants were bacterially expressed similarly to the wild-type protein and purified at small scales using the His-spin protein miniprep kit (Zymo Research). Expression and purity of the mutants were quantified by SDS−PAGE. Ubiquitination assays were performed in a 50 μL reaction buffer [50 mM Tris (pH 7.6), 4 mM ATP, 2 mM $MgCl_2$, and 1 mM DTT]. Reactions containing 1 μg of wild-type or mutant *Hs*CHIP, 100 ng of human E1 enzyme (Boston Biochem), 1 μg of UbcH5b, and 6 μg of bovine ubiquitin (Sigma) were incubated at 30 °C for 2 h and terminated by the addition of SDS−PAGE sample buffer. Western blotting with HRP-conjugated anti-ubiquitin (Santa Cruz Biotechnology) was used to identify ubiquitinated species.

NMR Spectroscopy. *Hs*CHIP-U and human ^{15}N-UbcH5b were dialyzed in 150 mM KCl, 20 mM potassium phosphate (pH 7.0), 10 μM $ZnCl_2$, and 10% D_2O. The sample concentration of ^{15}N-UbcH5b was 0.25 mM, and unlabeled *Hs*CHIP-U was added to give UbcH5b/CHIP ratios of 1:1 and 1:2. ^{15}N-^{1}H HSQC spectra were recorded at 25 °C on a Bruker Avance 600 MHz spectrometer equipped with a cryoprobe. Spectra were processed using NMRPipe (*57*) and visualized using NMRView (*58*). Peaks were assigned on the basis of the NMR structure of UbcH5b [PDB ID 1W4U; BioMagResBank code 6277 (*59*)]. Chemical-shift perturbations were calculated using the formula: $\Delta\delta_{total} = [\Delta\delta_{HN}^2 + (\Delta\delta_N/6.5)^2]^{1/2}$ (*60*). Titrations were also performed using unlabeled *Dr*CHIP-HU and gave qualitatively similar but lower-quality spectra with smaller chemical-shift perturbations, possibly because of limited precipitation or aggregation of the *Dr*CHIP-HU/UbcH5b complex (data not shown).

Structural Modeling. A model of a symmetric *Mm*CHIP dimer was constructed as follows: First, the U-box domain of the "unbroken" protomer in the structure of *Mm*CHIP (*49*) was superimposed onto its equivalent in the *Dr*CHIP-HU structure. Next, the TPR and helical linker domains of the "unbroken" protomer of *Mm*CHIP were superimposed as a unit onto the helical linker domain of *Dr*CHIP-HU. The relative positions of the *Mm*CHIP TPR and helical linker domains were not altered. The loop connecting the helical linker domain and the U-box of the resulting monomer was manually rebuilt in O (*55*) using the equivalent loop in *Dr*CHIP-HU as a guide. A homodimer was generated (by rotation around the 2-fold axis of the symmetric *Dr*CHIP-HU dimer) and minimized using CNS (*56*) to regularize backbone geometry and remove side-chain steric clashes.

A model of the CHIP−UbcH5b interaction surface was constructed by superimposing the *Dr*CHIP-HU and UbcH5b structures onto the structure of the c-Cbl RING/UbcH7 complex (*61*). The model was further minimized using CNS (*56*) to remove side-chain steric clashes.

RESULTS

Overall Structure of Zebrafish CHIP Helical Linker and U-Box Domains. We obtained crystals from a construct of zebrafish CHIP residues 112−284, containing the helical linker and U-box domains (termed *Dr*CHIP-HU in this paper). *Dr*CHIP-HU and full-length CHIP constructs were dimeric in solution, as estimated from gel-filtration chromatography (data not shown). *Dr*CHIP-HU crystallized in space group $P6_522$, with dimer interfaces coinciding with one of the crystallographic 2-fold axes (Figure 1). Dimerization buries ~1380 Å^2 on each monomer. In each homodimer, there are two distinct dimerization interfaces involving interactions between the two helical domains and between the two U-boxes, respectively.

The helical linker domain contains two long antiparallel helices (residues 130−164 and 184−204), which pack against each other through hydrophobic side-chain−side-chain interactions. These helices correspond to helices α7

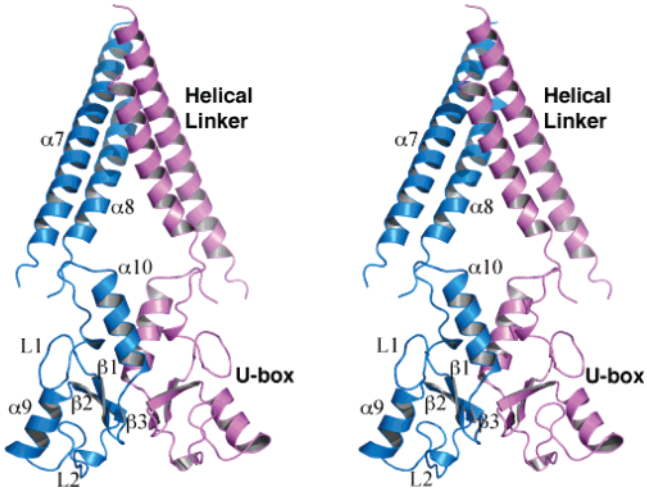

FIGURE 1: Stereoview of the *Dr*CHIP-HU dimer. The helical and U-box domains and secondary-structure elements are labeled. All molecular graphics in this and other figures were generated using PyMol (*73*).

and α8 of *Mm*CHIP, because the N-terminal TPR domain (not present in our structure) has six helices (*49*). Residues 112−126 and 165−183 did not show appreciable electron density, probably because they are flexible loops in our crystals. Helix α8 is followed by an extended region without standard secondary structure, which leads into the U-box domain and also makes contact with an extreme C-terminal segment of *Dr*CHIP-HU.

The *Dr*CHIP U-box domain adopts a characteristic fold observed in structures from pre-mRNA splicing factor Prp19, 2BAY (PDB ID 1N87); an armadillo repeat containing protein from *A. thaliana*, AtPUB14 (1T1H); and human ubiquitin conjugation factor E4A, UBE4A (1WGM) (*23*, *25*, *62*). The CHIP U-box main chain superimposes onto the other U-boxes with a root-mean-square deviation (rmsd) of 1.2−1.5 Å, with the major structural differences occurring in the N-terminal loops, the angle of the C-terminal helix (not present in the Prp19 U-box), and the lengths of the β-hairpin turns (Figure 2A). The N-terminal end of the U-box packs against the C-terminal helix. A long loop, L1, leads into a β hairpin that forms part of the central three-stranded β sheet. The second β strand leads into a central α helix (α9), which is followed by a second loop, L2. L2 is followed by a short α-helical turn and the short β3 strand of the central β sheet, leading to the C-terminal α helix (α10) and an unstructured C-terminal tail 8−9 residues in length.

Structural Details of the DrCHIP U-Box Domain. Two hydrogen-bonding networks restrict the conformations of loops L1 and L2 in the U-box. The first network restricts L1 with respect to the N terminus of α9. This network involves residues that are in positions similar to those occupied by four cysteines that coordinate one of the zinc ions of the c-Cbl RING domain (*61*) (Figure 2B). In other U-box structures, the position of the zinc is occupied by the side chain of an acidic residue at a position equivalent to C401 in c-Cbl. The acidic residue makes hydrogen bonds with two serines, located in positions equivalent to c-Cbl C384 and C404 (*61*) in most of the low-energy structures of the NMR ensembles in other U-box structures. In *Dr*CHIP, however, this residue (D234) is an integral part of a hydrogen-bonding network between α9 and a bulge at the C-terminal part of L1 (Figure 2C). The hairpin turn of L1 interacts with α9 through hydrogen bonding between S217 and D237. Surprisingly, we also observed an electron density located between the main-chain amides of I216, S217, and D234 that most likely corresponds to a chloride anion. No similar ion is observed in other U-box structures, and the chloride ion causes the L1 loop to pack more compactly against the rest of the domain in *Dr*CHIP-HU than in other U-box structures.

The second hydrogen-bonding network links the hairpin turn between the β1 and β2 strands with loop L2, as well as linking L2 with the C terminus of α9. This network approximates the second zinc-binding site of the c-Cbl RING domain (parts D and E of Figure 2). Residues corresponding to the RING zinc-liganding residues participate in extensive hydrogen bonding, organized around an aspartic acid side chain (D249). The network is supplemented by a hydrophobic interaction (I231/V251) in *Dr*CHIP that is also present in UBE4A but is absent from other U-box structures. The U-box and RING residues whose side chains participate in these two bonding networks are highlighted in Figure 2F.

The C-terminal U-box helix (α10) is involved in dimerization (see below) and is followed by an unstructured tail. The helix and tail pack against the extended segment located between the helical linker domain and the U-box, and the tail packs against the N terminus of α7, primarily through hydrophobic interactions. The packed side chains, along with the upper surface of loop L1, form a solvent-exposed hydrophobic pocket or groove (Figure 3). This pocket is also exposed in the full-length *Mm*CHIP structure (*49*) and may constitute a protein−protein interaction site.

Symmetric Dimerization of DrCHIP-HU and a Comparison with the MmCHIP Structure. Our crystal structure shows a symmetric dimer, with the dimer axis coinciding with one of the crystallographic axes. There are two dimerization interfaces formed by packing between the helical domains and between the U-box domains, respectively. The helical domain interactions that comprise the first dimerization interface are limited to approximately three turns of α7/α8, because the two helix pairs subtend an angle of ∼65°. The dimerization involves extensive hydrophobic packing, including a number of aromatic side chains (Figure 4A). The second dimerization interface is located between the U-box domains and is composed of a γ turn in the N-terminal portion of the domain, the hairpin turn of the central β sheet, and part of α10 (Figure 4B). The side chain of Y211 contacts V270 and A273 in the symmetry-related copy of α10, while M267 interacts with its symmetry-related counterpart. I226 and I262 from each monomer pack against the complementary pair of isoleucines. In addition, a hydrogen-bonding network is formed between the U-boxes through a symmetric interaction between N264 side chains, which are stabilized by hydrogen bonding between N264 and T232 within each U-box monomer.

Individually, the dimerization interfaces are similar in *Dr*CHIP-HU and *Mm*CHIP. In the *Mm*CHIP structure, however, the 2-fold axes of the two dimerization interfaces do not coincide, creating an asymmetric dimer (*49*). The position of the helical linker domain in our structure is intermediate between the positions of the linker domains in the two protomers of the *Mm*CHIP dimer structure (Figure 5A). In the *Mm*CHIP structure, the two helices of one linker

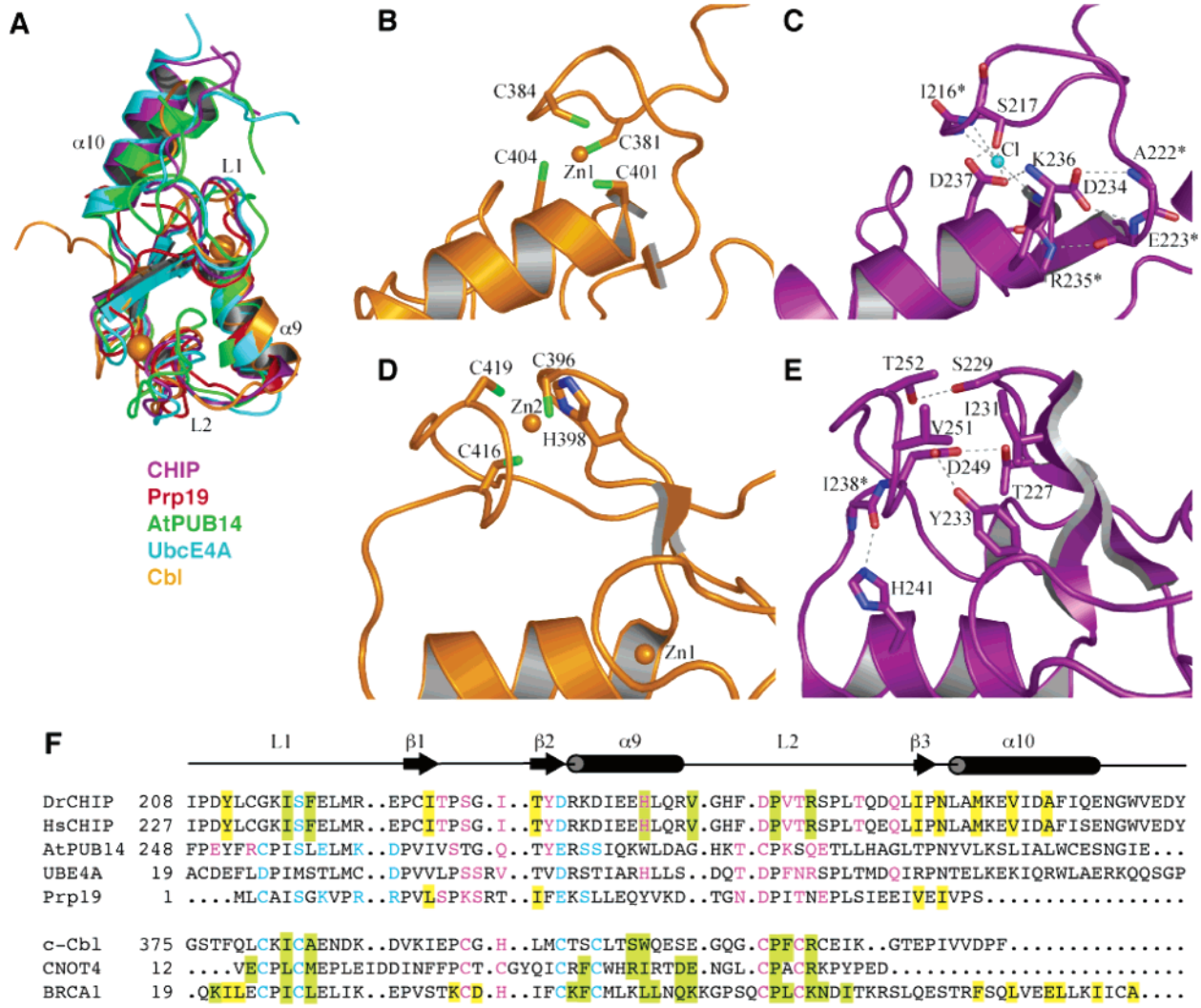

FIGURE 2: (A) Superimposition of the U-boxes from *Dr*CHIP, Prp19, AtPUB14, and UBE4A and the RING domain of c-Cbl. The two zinc atoms of the c-Cbl RING domain are shown as spheres. (B) Comparison of the first zinc-binding site of c-Cbl with (C) the equivalent region of the *Dr*CHIP U-box. Dotted lines indicate hydrogen bonds. Residues that participate in hydrogen bonding through main-chain atoms are marked with an asterisk, and their side chains are not shown. A chloride ion that interacts with the main-chain amide groups of I216, S217, and D234 is shown as a cyan sphere. (D) Comparison of the second zinc-binding site of c-Cbl with (E) the equivalent region of the *Dr*CHIP U-box. For clarity, only a subset of the long-range hydrogen bonds is shown. (F) Structure-based sequence alignment of U-boxes and representative RING domains. Residues whose side chains participate in the first hydrogen-bonding network (U-boxes) or zinc-binding site (RING domains) are colored cyan, and those with side chains participating in the second hydrogen-bonding network or zinc-binding site are colored magenta. Residues that participate in dimerization are shown on a yellow background (CHIP, Prp19, and BRCA1 sequences only). Residues that interact with UbcH5 (see Figure 6) or UbcH7 (Cbl only) are shown on a light-green background.

domain are almost parallel to the 2-fold axis between the U-box domains, while the other linker domain is at a ~65° angle. Helix α7 in the latter protomer is "broken" into two individual helices connected by an 8-residue unstructured segment (Figure 5A). The N-terminal portion of α7 interacts with the TPR domain in both *Mm*CHIP protomers, although the TPR domains are at different positions in each protomer. The *Dr*CHIP-HU linker domain structure more closely resembles the "unbroken" linker domain in the *Mm*CHIP structure, and the N terminus of α7 in our structure occupies a similar position as the homologous residues of α7 in the "unbroken" *Mm*CHIP linker domain.

We generated a model of a symmetric dimer of full-length CHIP (Figure 5B) by tilting the helical linker and TPR domains of the "unbroken" *Mm*CHIP protomer and superimposing the helical linker onto its *Dr*CHIP-HU counterpart. We then applied a rotation around the *Dr*CHIP-HU 2-fold axis to generate the second protomer of the symmetric dimer. No steric clashes are generated in either of these operations. The positions of the TPR domains relative to the helical linker domains were not adjusted. As in the "unbroken" protomer of the asymmetric *Mm*CHIP dimer, the TPR domains in the symmetric dimer interact solely with the helical linker domains and do not contact the U-box domains.

Identification of CHIP Residues That Interact with UbcH5. CHIP functions in protein degradation process in concert with E2 enzymes of the Ubc4/UbcH5 family. Members of this E2 family mediate the degradation of cytoplasmic proteins under stress conditions in yeast and higher eukaryotes (*63*). The three human members of the UbcH5 family, UbcH5a, UbcH5b, and UbcH5c, are highly homologous (*64*). A cluster of hydrophobic residues located on one side of RING and U-box domains have been suggested to form the binding site for E2 enzymes (*23*, *25*, *61*). The residues are located around the interface between the central α helix of the U-box and loops L1 and L2 and present a common face to the solvent.

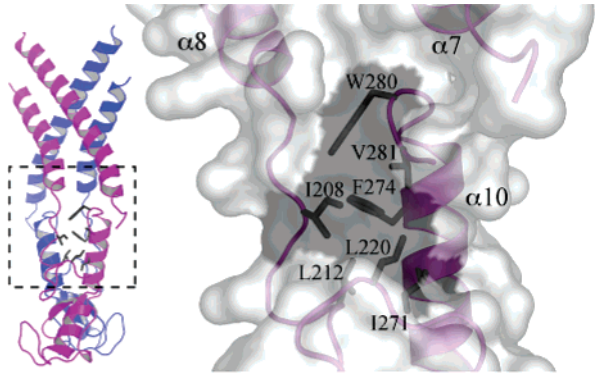

FIGURE 3: Solvent-accessible hydrophobic pocket on the surface of *Dr*CHIP-HU is located at the junction of the helical and U-box domains. The *Dr*CHIP-HU dimer is shown rotated approximately 90° about the vertical axis from its orientation in Figure 1. The portion of one monomer within the dashed box is shown as a closeup. Side chains of hydrophobic residues are shown and the corresponding areas of the transparent protein surface are shaded dark gray.

In the absence of another substrate, CHIP can catalyze autoubiquitination by UbcH5 family members (*65*). We mutated residues in full-length human CHIP with solvent-exposed side chains located in this region and used an in vitro assay to monitor ubiquitin chain formation and CHIP autoubiquitination in the presence of human UbcH5b (Figure 6A). Mutation of human CHIP I235, F237, H260, V264, or R272 to alanine abolished or greatly decreased the formation of high molecular-weight ubiquitinated species. When mapped onto the equivalent residues (I216, F218, H241, V245, and R253) in the *Dr*CHIP-HU structure (Figure 6B), these residues define a strip traversing loops L1 and L2 and including part of helix α9. The mutation of other nearby residues does not affect the ability of CHIP to catalyze UbcH5b ubiquitination activity, as observed in the *Hs*CHIP mutants D229A and V270A (D210 and V251 in *Dr*CHIP-HU).

Characterization of CHIP-Binding Site on UbcH5b by NMR Spectroscopy. The structure of human UbcH5b has been solved by NMR techniques (*59*). To characterize the binding site for CHIP on UbcH5b, we performed titrations of the U-box domain from human CHIP (*Hs*CHIP-U) against ^{15}N-labeled human UbcH5b. We used *Hs*CHIP-U rather than full-length zebrafish or human CHIP to limit the size of the complex and reduce the effects of line broadening. The human and zebrafish UbcH5b proteins are 98% identical in sequence; in addition, the U-boxes of human and zebrafish CHIP are 97% identical and 100% similar in sequence. We used the deposited chemical-shift assignments (BioMagResBank code 6277) to identify UbcH5b residues that may participate in the binding to CHIP (Figure 7A). UbcH5b residues exhibiting significant chemical-shift perturbations are located primarily on the N-terminal α1 helix and on a loop connecting a short helical turn with the α2 helix (Figure 7B). This loop has been termed the L7 loop in a recent survey of E2 enzymes (*66*). In addition to chemical-shift perturbations, one residue (S94) on loop L7 exhibits severe line broadening and disappears upon the binding of CHIP.

Residues exhibiting chemical-shift changes or line broadening form a contiguous region along one side of UbcH5b (Figure 7B). This region is similar to the interface of the E2 enzyme UbcH7 with the c-Cbl RING domain (*61*). We used

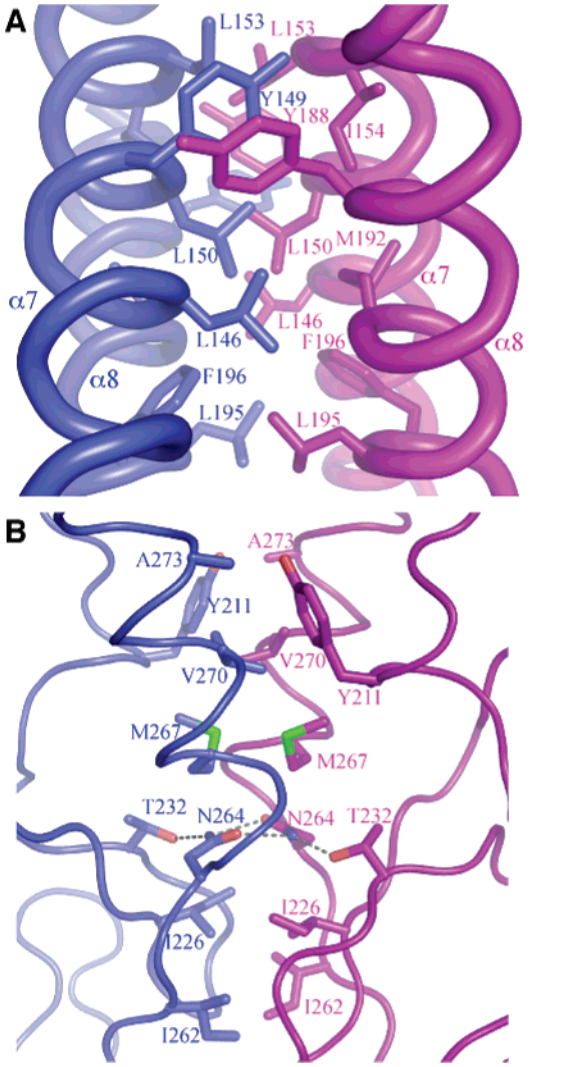

FIGURE 4: Dimerization interfaces of the *Dr*CHIP-HU dimer. Side chains making dimer contacts are shown in a stick representation. For clarity, the backbone is depicted in tube form. (A) Dimerization between the two helical domains. (B) Dimerization between the two U-boxes. Dotted lines indicate hydrogen bonds. T232 does not form a direct dimer contact but helps to orient the side chain of N264.

the c-Cbl/UbcH7 complex as a guide to construct a model of the CHIP/UbcH5b interface (Figure 7C), consistent with our mutagenesis and NMR data. The model suggests that F218 (F237 in *Hs*CHIP) contacts the aliphatic portions of several side chains on the UbcH5b α1 helix, while I216 (I235 in *Hs*CHIP), which is highly conserved in U-box and RING domains (Figure 2F), forms a contact with a conserved proline on the L7 loop of UbcH5b. The side chain of R253 (R272) interacts with several main-chain atoms on a helical turn that immediately precedes loop L7. In this arrangement, several CHIP residues on helix α9 may come in contact with UbcH5b loop L4, located behind L7. We did not observe many substantial chemical-shift perturbations of residues located near the tip of L4. In addition, the mutation of selected residues on α9, H241(H260 in *Hs*CHIP), and V245-(V264) reduced ubiquitination without eliminating it completely (Figure 6A). We thus modeled the complex so that only a proline at the tip of L4, residue P61, makes van der Waals contacts with the side chains of H241 and V245 (Figure 7C).

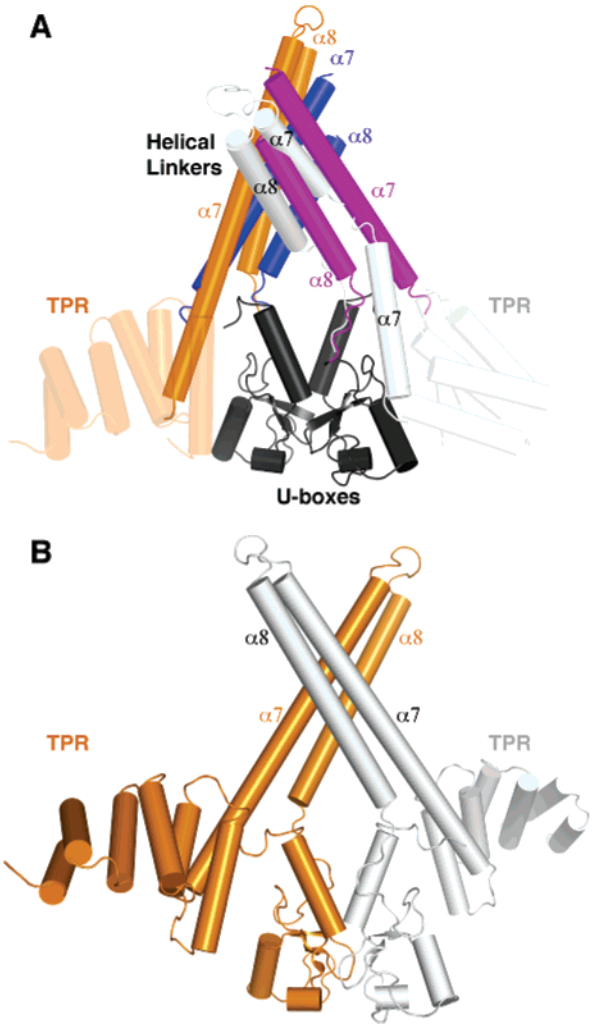

FIGURE 5: (A) Comparison between the symmetric *Dr*CHIP-HU dimer with the asymmetric dimer of *Mm*CHIP, on the basis of the superimposition of the U-box domains of each structure. The U-boxes superimpose almost exactly and are colored dark gray. Helices are shown as cylinders to emphasize their orientation. *Dr*CHIP-HU monomers are colored blue and purple as in other figures. The *Mm*CHIP protomer with a "broken" α7 helix is colored white, while the protomer with an "unbroken" α7 helix is shown in orange. The TPR domains, which were not present for our structure of *Dr*CHIP-HU, are faded. (B) Model of a symmetric full-length CHIP dimer, built by moving the helical linker and TPR domains of the "unbroken" protomer of *Mm*CHIP to superimpose onto the helical linker of *Dr*CHIP-HU.

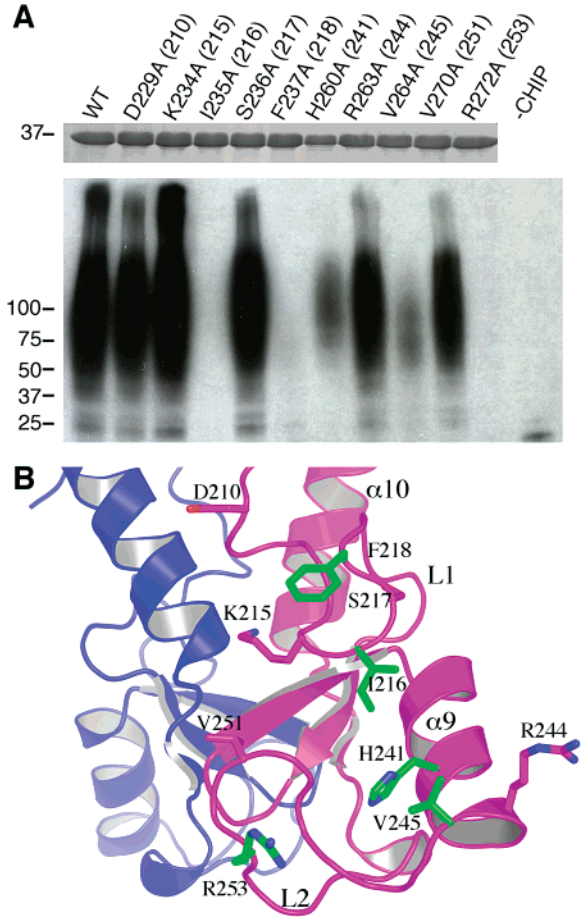

FIGURE 6: Identification of CHIP residues that interact with UbcH5b. (A) Results of the in vitro ubiquitination reaction containing wild-type or mutant human CHIP, E1 enzyme, human UbcH5b, and ubiquitin. (Lower panel) Western blotting for ubiquitin shows higher molecular-weight species corresponding to polyubiquitinated CHIP. Positions of molecular-weight standards (in kilodaltons) are marked. A reaction without CHIP (labeled "−CHIP") was used as a negative control. (Upper panel) Coomassie-stained gel showing comparable yields of wild-type and mutant CHIP after purification. The numbers in parentheses designate the zebrafish equivalent of the mutated residue. (B) Locations of equivalents of the mutated residues in the *Dr*CHIP U-box domain. Residues that decreased or eliminated ubiquitination when mutated are colored green; residues that had little or no effect when mutated are colored purple.

DISCUSSION

Does Full-Length CHIP Adopt Symmetric and Asymmetric Conformations? The major difference between our structure of *Dr*CHIP-HU and the recently published structure of human CHIP (*49*) is that the helical linker and U-box domains dimerize in a symmetric manner in our structure and share a common 2-fold axis. In contrast, the structure of full-length *Mm*CHIP shows an asymmetric dimer in which the arrangement of the TPR, helical linker, and U-box domains is different in each protomer (Figure 5A). In one protomer, helix α6 (of the TPR domain), as well as the N-terminal subhelix of the "broken" α7 helix, interacts with the U-box in such a manner as to block interactions with E2 enzymes (*49*). To stabilize the conformation of the "broken" protomer, the additional contacts made between the TPR domain and U-box domains compensate for the loss of intrahelical hydrogen bonding upon the "breaking" of helix α7 and the disordering of an 8−9-residue segment in the middle of this helix. Most of the individual interactions that mediate the interface between the U-box and α6/α7 are polar, suggesting that the interacting surfaces can be exposed to the solvent without penalty. Indeed, the corresponding surfaces are solvent-exposed in the other, "unbroken" protomer.

In our structure and in the "unbroken" *Mm*CHIP protomer, only a few residues of α7 interact with the U-box, and these interactions are limited to the unstructured extreme C terminus of the protein. The helical linker domain thus has substantial freedom of orientation relative to the U-box but remains fixed with respect to the TPR domain because of packing between α6 and α7. To form a full-length symmetric dimer similar to our structure of *Dr*CHIP-HU, tilting of the linker domain/TPR unit from its orientation in the "unbroken" protomer of *Mm*CHIP is required. Such a tilt is readily accommodated by the unstructured region connecting the

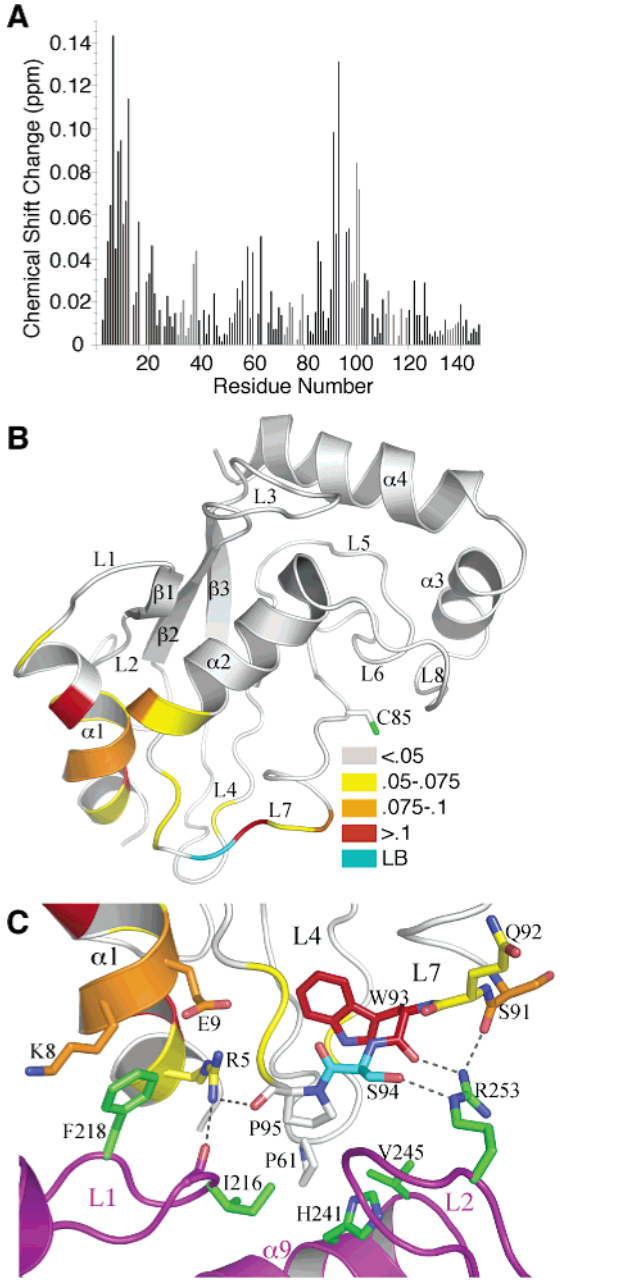

FIGURE 7: Investigation of the CHIP-binding surface on UbcH5b using NMR spectroscopy. (A) Average chemical-shift changes from ^{1}H-^{15}N HSQC spectra of free UbcH5b and a *Hs*CHIP-U-box/UbcH5b complex. (B) Structure of UbcH5b colored by chemical-shift perturbation. Cyan designates a residue, S94, whose ^{1}H-^{15}N resonance disappears in the complex because of line broadening ("LB"). The active-site cysteine residue (C85) that forms a thioester bond with ubiquitin is shown in a stick representation. Secondary-structure elements are labeled as in Winn et al. (*66*). (C) Model of the CHIP U-box/UbcH5b interface, on the basis of chemical-shift changes and the mutants shown in Figure 6. Selected residues that may participate in binding are shown in a stick representation. Carbons of UbcH5b residues are colored by a chemical-shift change, as in B. CHIP mutants that disrupt ubiquitination are shown with green carbons and are numbered according to the zebrafish sequence. Dotted lines indicate putative hydrogen bonds.

helical linker and U-box domains. Interdomain structural constraints are provided by the dimer interfaces (between the helical linker domains and between the U-boxes, respectively) and by the packing between the TPR and helical linker domains. Full-length *Dr*CHIP and mammalian CHIP should thus be able to adopt the symmetric arrangement observed in our structure of *Dr*CHIP-HU. We have modeled such a symmetric, full-length CHIP dimer in Figure 5B.

Zhang et al. used isothermal titration calorimetry to show that full-length *Mm*CHIP forms a 2:1 complex rather than a 2:2 complex with the E2 enzyme Ubc13, suggesting that one U-box in the dimer is blocked by the TPR domain of the same protomer and that the asymmetric dimer can exist in solution (*49*). While we cannot eliminate the possibility that the helical linker and U-box domains adopt a symmetric arrangement only upon deletion of the TPR domain, our model shows that the TPR domain can be accommodated in the context of a symmetric dimer. We suggest that the CHIP dimer may convert between symmetric and asymmetric conformations, possibly influenced by interactions with other proteins.

Dimerization in U-Box Ubiquitin Ligases. Dimerization is required for ubiquitination of chaperone substrates by CHIP (*18*, *26*). The CHIP U-box by itself dimerizes at the high concentrations required for crystallization, in the same configuration as observed in the *Dr*CHIP-HU and *Mm*CHIP structures (*49*). The Prp19 U-box also crystallizes as a dimer (*62*), and the U-box of AtPUB14 shows evidence of dimerization in solution at high concentrations (*23*). A subset of the residues involved in dimerization of the CHIP U-box fulfills the same function in these other U-boxes (Figure 2F). Our structure and that of *Mm*CHIP define a structural basis for U-box dimerization mediated by extensive nonpolar interactions involving both the N-terminal portion and C-terminal helix of the domain, as well as a buried hydrogen-bonding network involving N264.

The helical linker domain of CHIP may be necessary to enhance the propensity of the U-boxes to dimerize. A CHIP construct containing the TPR domain fused directly to the U-box does not dimerize or catalyze ubiquitination of model substrates. Similarly, a construct consisting solely of the helical linker domain has a dominant negative effect on full-length CHIP by forming nonfunctional heterodimers (*26*). Among other ubiquitin ligases, Prp19 has a coiled-coil tetramerization domain located C-terminal to its U-box, without which the Prp19 U-box dimerizes only weakly in solution (*62*). Similarly, dimerization of the RING domains in the heterodimeric BRCA1−BARD1 ubiquitin ligase is stabilized by interactions between N-terminal helices preceding the RING domains as well as C-terminal helices (*67*). Dimerization of U-box or RING domains into a rigid structural unit may be required for the proper functioning of ubiquitin ligases, even though the U-box or RING monomers can, in principle, interact with E2 enzymes individually. We are testing this hypothesis using CHIP mutants that disrupt the dimerization of the U-box domains without eliminating the interactions between the helical linker domains.

CHIP Interactions with UbcH5b Resemble RING/E2 and CHIP/Ubc13 Interactions. Members of the Ubc4/UbcH5 family of E2 enzymes are associated with the degradation of misfolded proteins in vivo and are "typical" E2 partners for CHIP in the context of Hsp70 or Hsp90 heterocomplexes. Using mutagenesis and NMR spectroscopy, we characterized the interaction between CHIP and UbcH5b. In our model based on the c-Cbl/UbcH7 complex, F218 on loop L1 and R253 on loop L2 of the U-box each anchor a side of UbcH5b by interacting with α1 and a helical turn at the N terminus

of the L7 loop, respectively (Figure 7C). Between these two residues, a hydrophobic side chain (I216) and a proline (P250) contact P95 of UbcH5b, which is highly conserved among E2 enzymes (*66*). This arrangement positions basic side chains on UbcH5b α1 to interact with main-chain atoms on loop L1 of the U-box. Additional weaker contacts are made between a proline (P61) at the tip of the UbcH5b L4 loop and aliphatic portions of two residues on the α9 helix of the U-box. These contacts define a minimal set of requirements for UbcH5b binding. Similar contacts are found in the c-Cbl/UbcH7 and *Mm*CHIP/Ubc13 crystal structures (*49*, *61*) and have been proposed for the interaction between UbcH5b and the RING finger of CNOT4 (*68*).

The UbcH5b residues involved in the interface with CHIP are largely conserved in Ubc13, which also functions as an E2 for CHIP (*49*). An exception is that P61 of UbcH5b is replaced by a methionine side chain in Ubc13, which makes more extensive van der Waals contacts with residues on α9 of the U-box. CHIP selectivity between UbcH5b and Ubc13 may additionally be governed by contextual factors such as subcellular localization rather than binding preference for one over the other. The CHIP residues that interact with UbcH5b are conserved in other U-boxes, with the exception of Prp19 and cyclophilin-4 (*21*). Interestingly, rather than interacting with members of the Ubc4/UbcH5 family, Prp19 catalyzes ubiquitination by Ubc3, while cyclophilin-4 is active with Ubc2B, Ubc3, or UbcH7 (*21*).

CONCLUSIONS

We have structurally characterized a novel symmetric dimer of *Dr*CHIP-HU that differs from the asymmetric dimer observed in the *Mm*CHIP structure. The structural constraints imposed by the helical linker and U-box dimerization interfaces can be accommodated in two ways, and we suggest that the symmetric and asymmetric dimers represent two different conformations of CHIP. We have also characterized the interaction surfaces between CHIP and UbcH5b and defined a minimal set of interactions that provide specificity between U-box-containing E3 ligases and the UbcH5 family of E2 enzymes.

CHIP interacts simultaneously with Hsp70 and with cochaperones, including Bag-1 (*27*, *69*), Bag-2 (*70*, *71*), and HspBP1 (*72*), with chaperone substrates, and with E2 enzymes. The interaction between CHIP and Hsp70 or Hsp90 within a chaperone heterocomplex may not be limited to the contact between the TPR domain and the heat-shock protein C-terminal ΦEEVD motifs. At least one paper has suggested that the helical linker domain is also required for the association between Hsp70 and CHIP (*18*). We have noted a solvent-exposed hydrophobic surface located at the junction between the helical linker and U-box domains (Figure 3). Other putative protein−protein interaction sites on the CHIP dimer await characterization. CHIP catalyzes ubiquitination through diverse lysines on ubiquitin in a substrate-dependent manner and ubiquitinates not only chaperone substrates but also the chaperones and cochaperones. For example, CHIP modifies Bag-1 with a K11-linked chain (*69*), while Hsc70 itself is modified with K29- or K63-linked chains (*65*). The ability of CHIP to access chaperone substrates and cochaperones and to catalyze different modes of ubiquitination must be related to the relative positions of CHIP and the other components of a chaperone heterocomplex. It will thus be important to further characterize the structure of CHIP and its interacting partners in the context of such chaperone complexes to explain the basis of CHIP specificity and function and to define the role of CHIP dimerization.

REFERENCES

1. Young, J. C., Agashe, V. R., Siegers, K., and Hartl, F. U. (2004) Pathways of chaperone-mediated protein folding in the cytosol, *Nat. Rev. Mol. Cell Biol. 5*, 781−791.
2. Mayer, M. P., and Bukau, B. (2005) Hsp70 chaperones: Cellular functions and molecular mechanism, *Cell Mol. Life Sci. 62*, 670−684.
3. Wegele, H., Muller, L., and Buchner, J. (2004) Hsp70 and Hsp90−A relay team for protein folding, *Rev. Physiol. Biochem. Pharmacol. 151*, 1−44.
4. Terasawa, K., Minami, M., and Minami, Y. (2005) Constantly updated knowledge of Hsp90, *J. Biochem. 137*, 443−447.
5. Hatakeyama, S., Matsumoto, M., Yada, M., and Nakayama, K. I. (2004) Interaction of U-box-type ubiquitin-protein ligases (E3s) with molecular chaperones, *Genes Cells 9*, 533−548.
6. Cyr, D. M., Hohfeld, J., and Patterson, C. (2002) Protein quality control: U-box-containing E3 ubiquitin ligases join the fold, *Trends Biochem. Sci. 27*, 368−375.
7. McDonough, H., and Patterson, C. (2003) CHIP: A link between the chaperone and proteasome systems, *Cell Stress Chaperones 8*, 303−308.
8. Murata, S., Chiba, T., and Tanaka, K. (2003) CHIP: A quality-control E3 ligase collaborating with molecular chaperones, *Int. J. Biochem. Cell Biol. 35*, 572−578.
9. Wiederkehr, T., Bukau, B., and Buchberger, A. (2002) Protein turnover: A CHIP programmed for proteolysis, *Curr. Biol. 12*, R26−R28.
10. Wickner, S., Maurizi, M. R., and Gottesman, S. (1999) Posttranslational quality control: Folding, refolding, and degrading proteins, *Science 286*, 1888−1893.
11. Hatakeyama, S., and Nakayama, K. I. (2003) Ubiquitylation as a quality control system for intracellular proteins, *J. Biochem. 134*, 1−8.
12. Hershko, A., and Ciechanover, A. (1998) The ubiquitin system, *Annu. Rev. Biochem. 67*, 425−479.
13. Pickart, C. M., and Eddins, M. J. (2004) Ubiquitin: Structures, functions, mechanisms, *Biochim. Biophys. Acta 1695*, 55−72.
14. Glickman, M. H., and Ciechanover, A. (2002) The ubiquitin-proteasome proteolytic pathway: Destruction for the sake of construction, *Physiol. Rev. 82*, 373−428.
15. Robinson, P. A., and Ardley, H. C. (2004) Ubiquitin-protein ligases, *J. Cell Sci. 117*, 5191−5194.
16. Ardley, H. C., and Robinson, P. A. (2005) E3 ubiquitin ligases, *Essays Biochem. 41*, 15−30.
17. Connell, P., Ballinger, C. A., Jiang, J., Wu, Y., Thompson, L. J., Hohfeld, J., and Patterson, C. (2001) The co-chaperone CHIP regulates protein triage decisions mediated by heat-shock proteins, *Nat. Cell Biol. 3*, 93−96.
18. Ballinger, C. A., Connell, P., Wu, Y., Hu, Z., Thompson, L. J., Yin, L. Y., and Patterson, C. (1999) Identification of CHIP, a novel tetratricopeptide repeat-containing protein that interacts with heat shock proteins and negatively regulates chaperone functions, *Mol. Cell. Biol. 19*, 4535−4545.
19. Wu, S. J., Liu, F. H., Hu, S. M., and Wang, C. (2001) Different combinations of the heat-shock cognate protein 70 (hsc70) C-terminal functional groups are utilized to interact with distinct tetratricopeptide repeat-containing proteins, *Biochem. J. 359*, 419−426.
20. Hatakeyama, S., and Nakayama, K. I. (2003) U-box proteins as a new family of ubiquitin ligases, *Biochem. Biophys. Res. Commun. 302*, 635−645.
21. Hatakeyama, S., Yada, M., Matsumoto, M., Ishida, N., and Nakayama, K. I. (2001) U box proteins as a new family of ubiquitin-protein ligases, *J. Biol. Chem. 276*, 33111−33120.
22. Hoppe, T. (2005) Multiubiquitylation by E4 enzymes: "One size" doesn't fit all, *Trends Biochem. Sci. 30*, 183−187.
23. Andersen, P., Kragelund, B. B., Olsen, A. N., Larsen, F. H., Chua, N. H., Poulsen, F. M., and Skriver, K. (2004) Structure and biochemical function of a prototypical *Arabidopsis* U-box domain, *J. Biol. Chem. 279*, 40053−40061.

24. Aravind, L., and Koonin, E. V. (2000) The U box is a modified RING finger−A common domain in ubiquitination, *Curr. Biol. 10*, R132−R134.
25. Ohi, M. D., Vander Kooi, C. W., Rosenberg, J. A., Chazin, W. J., and Gould, K. L. (2003) Structural insights into the U-box, a domain associated with multi-ubiquitination, *Nat. Struct. Biol. 10*, 250−255.
26. Nikolay, R., Wiederkehr, T., Rist, W., Kramer, G., Mayer, M. P., and Bukau, B. (2004) Dimerization of the human E3 ligase CHIP via a coiled-coil domain is essential for its activity, *J. Biol. Chem. 279*, 2673−2678.
27. Demand, J., Alberti, S., Patterson, C., and Hohfeld, J. (2001) Cooperation of a ubiquitin domain protein and an E3 ubiquitin ligase during chaperone/proteasome coupling, *Curr. Biol. 11*, 1569−1577.
28. He, B., Bai, S., Hnat, A. T., Kalman, R. I., Minges, J. T., Patterson, C., and Wilson, E. M. (2004) An androgen receptor NH_2-terminal conserved motif interacts with the COOH terminus of the Hsp70-interacting protein (CHIP), *J. Biol. Chem. 279*, 30643−30653.
29. Tateishi, Y., Kawabe, Y., Chiba, T., Murata, S., Ichikawa, K., Murayama, A., Tanaka, K., Baba, T., Kato, S., and Yanagisawa, J. (2004) Ligand-dependent switching of ubiquitin-proteasome pathways for estrogen receptor, *EMBO J. 23*, 4813−4823.
30. Cardozo, C. P., Michaud, C., Ost, M. C., Fliss, A. E., Yang, E., Patterson, C., Hall, S. J., and Caplan, A. J. (2003) C-terminal Hsp-interacting protein slows androgen receptor synthesis and reduces its rate of degradation, *Arch. Biochem. Biophys. 410*, 134−140.
31. Wang, X., and DeFranco, D. B. (2005) Alternative effects of the ubiquitin-proteasome pathway on glucocorticoid receptor down-regulation and transactivation are mediated by CHIP, an E3 ligase, *Mol. Endocrinol. 19*, 1474−1482.
32. Xu, W., Marcu, M., Yuan, X., Mimnaugh, E., Patterson, C., and Neckers, L. (2002) Chaperone-dependent E3 ubiquitin ligase CHIP mediates a degradative pathway for c-ErbB2/Neu, *Proc. Natl. Acad. Sci. U.S.A. 99*, 12847−12852.
33. Zhou, P., Fernandes, N., Dodge, I. L., Reddi, A. L., Rao, N., Safran, H., DiPetrillo, T. A., Wazer, D. E., Band, V., and Band, H. (2003) ErbB2 degradation mediated by the co-chaperone protein CHIP, *J. Biol. Chem. 278*, 13829−13837.
34. Xin, H., Xu, X., Li, L., Ning, H., Rong, Y., Shang, Y., Wang, Y., Fu, X. Y., and Chang, Z. (2005) CHIP controls the sensitivity of transforming growth factor-β signaling by modulating the basal level of Smad3 through ubiquitin-mediated degradation, *J. Biol. Chem. 280*, 20842−20850.
35. Li, L., Xin, H., Xu, X., Huang, M., Zhang, X., Chen, Y., Zhang, S., Fu, X. Y., and Chang, Z. (2004) CHIP mediates degradation of Smad proteins and potentially regulates Smad-induced transcription, *Mol. Cell. Biol. 24*, 856−864.
36. Li, R. F., Zhang, F., Lu, Y. J., and Sui, S. F. (2005) Specific interaction between Smad1 and CHIP: A surface plasmon resonance study, *Colloids Surf., B 40*, 133−136.
37. Esser, C., Scheffner, M., and Hohfeld, J. (2005) The chaperone-associated ubiquitin ligase CHIP is able to target p53 for proteasomal degradation, *J. Biol. Chem. 280*, 27443−27448.
38. Timsit, Y. E., Miller, S. L., Mohney, R. P., and O'Bryan, J. P. (2005) The U-box ligase carboxyl-terminus of Hsc 70-interacting protein ubiquitylates Epsin, *Biochem. Biophys. Res. Commun. 328*, 550−559.
39. Shin, Y., Klucken, J., Patterson, C., Hyman, B. T., and McLean, P. J. (2005) The co-chaperone carboxyl terminus of Hsp70-interacting protein (CHIP) mediates α-synuclein degradation decisions between proteasomal and lysosomal pathways, *J. Biol. Chem. 280*, 23727−23734.
40. Miller, V. M., Nelson, R. F., Gouvion, C. M., Williams, A., Rodriguez-Lebron, E., Harper, S. Q., Davidson, B. L., Rebagliati, M. R., and Paulson, H. L. (2005) CHIP suppresses polyglutamine aggregation and toxicity in vitro and in vivo, *J. Neurosci. 25*, 9152−9161.
41. Jana, N. R., Dikshit, P., Goswami, A., Kotliarova, S., Murata, S., Tanaka, K., and Nukina, N. (2005) Co-chaperone CHIP associates with expanded polyglutamine protein and promotes their degradation by proteasomes, *J. Biol. Chem. 280*, 11635−11640.
42. Hatakeyama, S., Matsumoto, M., Kamura, T., Murayama, M., Chui, D. H., Planel, E., Takahashi, R., Nakayama, K. I., and Takashima, A. (2004) U-box protein carboxyl terminus of Hsc70-interacting protein (CHIP) mediates poly-ubiquitylation preferentially on four-repeat Tau and is involved in neurodegeneration of tauopathy, *J. Neurochem. 91*, 299−307.
43. Petrucelli, L., Dickson, D., Kehoe, K., Taylor, J., Snyder, H., Grover, A., De Lucia, M., McGowan, E., Lewis, J., Prihar, G., Kim, J., Dillmann, W. H., Browne, S. E., Hall, A., Voellmy, R., Tsuboi, Y., Dawson, T. M., Wolozin, B., Hardy, J., and Hutton, M. (2004) CHIP and Hsp70 regulate tau ubiquitination, degradation and aggregation, *Hum. Mol. Genet. 13*, 703−714.
44. Shimura, H., Schwartz, D., Gygi, S. P., and Kosik, K. S. (2004) CHIP-Hsc70 complex ubiquitinates phosphorylated tau and enhances cell survival, *J. Biol. Chem. 279*, 4869−4876.
45. Choi, J. S., Cho, S., Park, S. G., Park, B. C., and Lee do, H. (2004) Co-chaperone CHIP associates with mutant Cu/Zn-superoxide dismutase proteins linked to familial amyotrophic lateral sclerosis and promotes their degradation by proteasomes, *Biochem. Biophys. Res. Commun. 321*, 574−583.
46. Urushitani, M., Kurisu, J., Tateno, M., Hatakeyama, S., Nakayama, K., Kato, S., and Takahashi, R. (2004) CHIP promotes proteasomal degradation of familial ALS-linked mutant SOD1 by ubiquitinating Hsp/Hsc70, *J. Neurochem. 90*, 231−244.
47. Meacham, G. C., Patterson, C., Zhang, W., Younger, J. M., and Cyr, D. M. (2001) The Hsc70 co-chaperone CHIP targets immature CFTR for proteasomal degradation, *Nat. Cell Biol. 3*, 100−105.
48. Younger, J. M., Ren, H. Y., Chen, L., Fan, C. Y., Fields, A., Patterson, C., and Cyr, D. M. (2004) A foldable CFTR{δ}F508 biogenic intermediate accumulates upon inhibition of the Hsc70−CHIP E3 ubiquitin ligase, *J. Cell Biol. 167*, 1075−1085.
49. Zhang, M., Windheim, M., Roe, S. M., Peggie, M., Cohen, P., Prodromou, C., and Pearl, L. H. (2005) Chaperoned ubiquitylation-crystal structures of the CHIP U box E3 ubiquitin ligase and a CHIP−Ubc13-Uev1a complex, *Mol. Cell 20*, 525−538.
50. Kapust, R. B., Tozser, J., Fox, J. D., Anderson, D. E., Cherry, S., Copeland, T. D., and Waugh, D. S. (2001) Tobacco etch virus protease: Mechanism of autolysis and rational design of stable mutants with wild-type catalytic proficiency, *Protein Eng. 14*, 993−1000.
51. Sheffield, P., Garrard, S., and Derewenda, Z. (1999) Overcoming expression and purification problems of RhoGDI using a family of "parallel" expression vectors, *Protein Expression Purif. 15*, 34−39.
52. Pflugrath, J. W. (1999) The finer things in X-ray diffraction data collection, *Acta Crystallogr., Sect. D: Biol. Crystallogr. 55*, 1718−1725.
53. Terwilliger, T. C. (2000) Maximum-likelihood density modification, *Acta Crystallogr., Sect. D: Biol. Crystallogr. 56*, 965−972.
54. Terwilliger, T. C., and Berendzen, J. (1999) Automated MAD and MIR structure solution, *Acta Crystallogr., Sect. D: Biol. Crystallogr. 55*, 849−861.
55. Jones, T. A., Zou, J. Y., Cowan, S. W., and Kjeldgaard, M. (1991) Improved methods for building protein models in electron density maps and the location of errors in these models, *Acta Crystallogr., Sect. A: Found. Crystallogr. 47*, 110−119.
56. Brunger, A. T., Adams, P. D., Clore, G. M., DeLano, W. L., Gros, P., Grosse-Kunstleve, R. W., Jiang, J. S., Kuszewski, J., Nilges, M., Pannu, N. S., Read, R. J., Rice, L. M., Simonson, T., and Warren, G. L. (1998) Crystallography and NMR system: A new software suite for macromolecular structure determination, *Acta Crystallogr., Sect. D: Biol. Crystallogr. 54*, 905−921.
57. Delaglio, F., Grzesiek, S., Vuister, G. W., Zhu, G., Pfeifer, J., and Bax, A. (1995) NMRPipe: A multidimensional spectral processing system based on UNIX pipes, *J. Biomol. NMR 6*, 277−293.
58. Johnson, B. A. (2004) Using NMRView to visualize and analyze the NMR spectra of macromolecules, *Methods Mol. Biol. 278*, 313−352.
59. Houben, K., Dominguez, C., van Schaik, F. M., Timmers, H. T., Bonvin, A. M., and Boelens, R. (2004) Solution structure of the ubiquitin-conjugating enzyme UbcH5B, *J. Mol. Biol. 344*, 513−526.
60. Mulder, F. A., Schipper, D., Bott, R., and Boelens, R. (1999) Altered flexibility in the substrate-binding site of related native and engineered high-alkaline Bacillus subtilisins, *J. Mol. Biol. 292*, 111−123.
61. Zheng, N., Wang, P., Jeffrey, P. D., and Pavletich, N. P. (2000) Structure of a c-Cbl−UbcH7 complex: RING domain function in ubiquitin-protein ligases, *Cell 102*, 533−539.
62. Vander Kooi, C. W., Ohi, M. D., Rosenberg, J. A., Oldham, M. L., Newcomer, M. E., Gould, K. L., and Chazin, W. J. (2006)

The Prp19 U-box crystal structure suggests a common dimeric architecture for a class of oligomeric E3 ubiquitin ligases, *Biochemistry 45*, 121−130.
63. Seufert, W., and Jentsch, S. (1990) Ubiquitin-conjugating enzymes UBC4 and UBC5 mediate selective degradation of short-lived and abnormal proteins, *EMBO J. 9*, 543−550.
64. Jensen, J. P., Bates, P. W., Yang, M., Vierstra, R. D., and Weissman, A. M. (1995) Identification of a family of closely related human ubiquitin conjugating enzymes, *J. Biol. Chem. 270*, 30408−30414.
65. Jiang, J., Ballinger, C. A., Wu, Y., Dai, Q., Cyr, D. M., Hohfeld, J., and Patterson, C. (2001) CHIP is a U-box-dependent E3 ubiquitin ligase: Identification of Hsc70 as a target for ubiquitylation, *J. Biol. Chem. 276*, 42938−42944.
66. Winn, P. J., Religa, T. L., Battey, J. N., Banerjee, A., and Wade, R. C. (2004) Determinants of functionality in the ubiquitin conjugating enzyme family, *Structure 12*, 1563−1574.
67. Brzovic, P. S., Rajagopal, P., Hoyt, D. W., King, M. C., and Klevit, R. E. (2001) Structure of a BRCA1−BARD1 heterodimeric RING−RING complex, *Nat. Struct. Biol. 8*, 833−837.
68. Dominguez, C., Bonvin, A. M., Winkler, G. S., van Schaik, F. M., Timmers, H. T., and Boelens, R. (2004) Structural model of the UbcH5B/CNOT4 complex revealed by combining NMR, mutagenesis, and docking approaches, *Structure 12*, 633−644.
69. Alberti, S., Demand, J., Esser, C., Emmerich, N., Schild, H., and Hohfeld, J. (2002) Ubiquitylation of BAG-1 suggests a novel regulatory mechanism during the sorting of chaperone substrates to the proteasome, *J. Biol. Chem. 277*, 45920−45927.
70. Dai, Q., Qian, S. B., Li, H. H., McDonough, H., Borchers, C., Huang, D., Takayama, S., Younger, J. M., Ren, H. Y., Cyr, D. M., and Patterson, C. (2005) Regulation of the cytoplasmic quality control protein degradation pathway by BAG2, *J. Biol. Chem. 280*, 38673−38681.
71. Arndt, V., Daniel, C., Nastainczyk, W., Alberti, S., and Hohfeld, J. (2005) BAG-2 acts as an inhibitor of the chaperone-associated ubiquitin ligase CHIP, *Mol. Biol. Cell 16*, 5891−5900.
72. Alberti, S., Bohse, K., Arndt, V., Schmitz, A., and Hohfeld, J. (2004) The cochaperone HspBP1 inhibits the CHIP ubiquitin ligase and stimulates the maturation of the cystic fibrosis transmembrane conductance regulator, *Mol. Biol. Cell 15*, 4003−4010.
73. DeLano, W. L. (2002) *The PyMol User's Manual*, DeLano Scientific, San Carlos, CA.

BI0601508